ELSEVIER

Physica C 319 (1999) 189–196

PHYSICA C

Point-contact study of the magnetic superconductor $HoNi_2B_2C$

L.F. Rybaltchenko [a,b], A.G.M. Jansen [a,*], P. Wyder [a], L.V. Tjutrina [b], P.C. Canfield [c], C.V. Tomy [d], D.McK. Paul [d]

[a] *Grenoble High Magnetic Field Laboratory, Max-Planck-Institut für Festkörperforschung and Centre National de la Recherche Scientifique, B.P. 166, F-38042 Grenoble Cedex 9, France*

[b] *B. Verkin Institute for Low Temperature Physics and Engineering, Academy of Sciences of Ukraine, 310164 Kharkiv, Ukraine*

[c] *Ames Laboratory, Iowa State University, Ames, IA 50011, USA*

[d] *Department of Physics, University of Warwick, Coventry CV4 7AL, UK*

Received 27 November 1998; received in revised form 8 March 1999; accepted 1 April 1999

Abstract

Point contacts (PC) based on the magnetic superconductor $HoNi_2B_2C$ with a superconducting onset temperature $T_c \sim 8.5$ K have been investigated in order to determine the temperature and magnetic field dependences of the superconducting order parameter. The temperature dependence of the order parameter satisfies the Bardeen–Cooper–Schrieffer (BCS) theory only below the BCS transition temperature $T_c^{BCS} = 5.5$–5.8 K, which exceeds slightly the Néel temperature $T_N \sim 5.0$ K. At higher temperatures, above T_N, the PC spectra $dV/dI(V)$ indicate an anomalous, most likely gapless, superconducting state. At magnetic fields well below H_{c2}, a considerable increase ($\sim 30\%$) in the characteristic voltage of the gap-related structure in the PC spectra is observed which points to an improved spin alignment with a decreasing influence of the pair breaking in modest fields.

PACS: 74.70.Ad; 74.80.Fp

Keywords: Magnetic superconductors; Borocarbides; Point contacts; Order parameter

1. Introduction

Among the magnetic superconductors of the borocarbide family $ReNi_2B_2C$ (Re—rare-earth element) [1], $HoNi_2B_2C$ marked by a complex magnetic structure [2,3] is of particular interest because of the strong anomalies in the superconducting characteristics [4]. Generally, superconductivity readily coexists with an antiferromagnetic (AFM) state (with some reduction of the pairing strength) due to a full compensation of the magnetic moments on the scale of the superconducting correlation length ξ. In $HoNi_2B_2C$, the AFM structure below the Néel temperature $T_N \sim 5.0$ K [5] consists of ordered Ho spins, ferromagnetically (FM) aligned in the Ho–C planes and antiferromagnetically coupled along the *c*-axis.

However, magnetic ordering persists in this compound above T_N, below a not yet well established temperature T_m. According to one neutron-scattering study [3], the magnetic order sets in already slightly

* Corresponding author. Tel.: +33-476-88-1058; Fax: +33-476-85-5610; E-mail: ljansen@labs.polycnrs-gr.fr

0921-4534/99/$ - see front matter
PII: S0921-4534(99)00282-8

below the superconducting critical temperature $T_c \sim 8.5$ K. Other neutron data reveal that this ordering starts at $T_m \sim 6.0$ K, i.e., closer to T_N [2]. Thermodynamic data, based on specific heat and magnetization measurements, confirm the latter value [5,6]. The elevated value for T_m given in Ref. [3] could be associated with a large broadening of the magnetic transition. In this magnetic phase above T_N, the in-plane ordered Ho spins are turned away from the AFM configuration by an angle $\sim 17°$ between adjacent planes, forming a spiral structure along the *c*-axis which results in a net FM component on a macroscopic scale. Moreover, independently of such an ordered structure below T_m, the spin–flip scattering may affect the superconductivity in $HoNi_2B_2C$ in the whole temperature range between T_N and T_c. If these pair-breaking effects are sufficiently strong a gapless state of superconductivity can result [7,8]. It should be noted that similar long-wave-length nonuniform spiral structure can arise in FM superconductors in order to approach a maximal compensation of the magnetic moments on the ξ scale because in a uniform case a simple coexistence of ferromagnetism and superconductivity is excluded due to their antagonistic character (for a review, see Ref. [7] and references therein).

In our earlier point-contact (PC) investigations of polycrystalline $HoNi_2B_2C$ [9], we have found that below T_N the superconducting PC characteristics resemble the conventional type of Andreev reflection spectra, whereas at higher temperatures very strong anomalies are observed. Therefore, the presence of two distinct superconducting states in this compound has been proposed. In the present work, we have extended our PC investigations of $HoNi_2B_2C$ with special emphasis on the temperature and magnetic field dependences of the superconducting order parameter. Only at low temperatures, below $\sim T_N$, the PC spectra (first derivatives $dV/dI(V)$ of the current–voltage characteristics) can be properly fitted to the appropriate Blonder–Tinkham–Klapwijk (BTK) theory for a normal metal–superconductor contact with a BCS superconductor. The deduced temperature dependence of the superconducting order parameter $\Delta(T)$ is close to the Bardeen–Cooper–Schrieffer (BCS) theory. At higher temperatures, the character of the spectra suggests a gapless-type superconductivity. In magnetic fields well below H_{c2}, a surprising increase of the gap parameter is observed which could point to a local spin alignment near the Ho sites with reduced pair-breaking.

2. Experimental details

The PC measurements were performed on $HoNi_2B_2C$, both polycrystalline and single-crystal samples, from 1.4 to 10 K in magnetic fields up to 10 T. The polycrystalline samples, used also in our previous experiments [9,10], were prepared by arc melting and showed the onset of superconductivity at $T_c \sim 8.7$ K with a transition width $\Delta T_c \sim 1.5$ K. The single crystals were grown in the form of thin plates by the Ni_2B flux method and had practically the same T_c value, but ΔT_c was about three times smaller [5]. According to X-ray examinations, both types of samples did not contain impurity phases. Among many tens of contacts investigated, most of them revealed T_c between 8.5 and 8.7 K in accordance with the bulk sample characteristics. On rare contacts, T_c could decrease by a few 0.1 K down to 8.2 K in individual cases. Since the T_c variation did not correlate with the contact resistance (i.e., with the contact size), this variation cannot be the consequence of a local pressure effect but is rather a signature of inhomogeneous superconducting properties over the sample volume.

The point contacts were established at 4.2 K by a gentle touch of a Ag needle as a counter electrode to a fresh superconducting electrode surface, prepared by breaking the sample just before immersing the sample holder into liquid He. For the broken plate-like single crystals, the contacts were adjusted with the contact axis parallel to the *a*–*b* plane. However, for the single-crystal based contacts with the contact axis parallel to the crystallographic *c*-axis, i.e., oriented normal of the plate surface, the natural untreated surface was probed. For these measurements, we have chosen the plates with a flat mirror-like surface. The relatively large size (~ 0.5 mm) of the crystallites in the polycrystalline samples ensured a high probability to probe single-crystalline regions although of undefined crystallographic orientation. A thin bronze wire was used as a spring in order to avoid a strong pressure of the Ag needle on the contact area. The point-contact spectra $dV/dI(V)$

were recorded by standard current-modulation techniques.

Typical contact resistances R at $V \gg \Delta/e$, corresponding to the normal-state resistance, ranged between 1 and 10 Ω. An indication for the corresponding contact sizes (radius d) can be found from the Wexler formula $R \approx \rho/2d + 4\rho l/3\pi d^2$ (l is the electron mean free path) [11] using the values for the bulk residual resistivity $\rho \sim 4$ μΩ cm and the product $\rho l \sim 4 \times 10^{-12}$ Ω cm^2 [6]. For the above given range of contact resistances one obtains contact radii $d \sim 5$–50 nm. The estimated d values provide a magnetic-field penetration into the whole contact area (the penetration depth $\lambda_L(0) \sim 100$ nm). In general, the data obtained on different contact resistances were identical, but in order to have a better mechanical and electrical stability of the contacts during the measurements the low ohmic contacts were investigated preferentially.

3. Temperature dependence of order parameter

Fig. 1 represents a typical set of the $dV/dI(V)$ spectra of a single crystal $HoNi_2B_2C$ based contact, with the contact axis directed along *ab*-plane, measured over a wide temperature range. As is seen, a standard double-minimum structure, which can be related to the superconducting BCS-gap, originates only below 5.8 K whereas the superconductivity sets in already at $T_c \sim 8.7$ K. Similar spectra have been reproducibly registered for a perpendicular-to-the-plane contact-axis direction which confirms the isotropic electronic structure of this compound. We note that in our previous PC investigations of polycrystalline $HoNi_2B_2C$ [9,10], the $dV/dI(V)$ spectra were very similar to those presented in Fig. 1, although good-quality Andreev-reflection spectra occurred significantly less often than in the single-crystal experiments.

The strong deviation of the Andreev-reflection spectra above T_N from the expected ones for conventional superconductors, seen in the same way on single-crystal and polycrystal based contacts, points to an essential modification of the superconducting state in this temperature range which, evidently, is not associated with an inhomogeneous distribution of superconducting properties over the contact area.

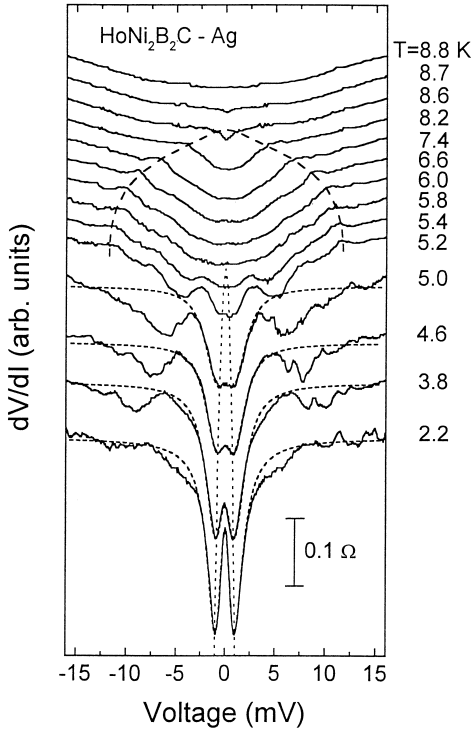

Fig. 1. A set of $dV/dI(V)$ characteristics for a point contact between single crystal $HoNi_2B_2C$ and Ag ($R(10\text{ mV}) \simeq 1.3$ Ω) with the contact axis oriented along the *ab*-plane. For clarity the curves are shifted vertically. Temperatures are indicated near each curve. The dashed and dotted lines show the temperature evolution of superconducting features in different temperature regions. Below 5.7 K a genuine BCS-state develops as indicated by the BTK fit of the data (short-dashed curves) with $\Delta(0) = 0.90$ meV. For the BTK curves at 2.2, 3.8, and 4.6 K: $\Gamma = 0.51$ meV and $Z = 0.60$; for the BTK curve at 5.0 K: $\Gamma = 0.60$ meV and $Z = 0.60$.

This unusual phenomenon may be explained by a pair-breaking influence of the incommensurate spiral spin structure found above T_N in neutron investigations [2,3]. Namely, this spin structure is probably responsible for the quasi-reentrance of the normal state, i.e., a partial suppression of superconductivity around T_N as seen in resistivity and magnetization data [4,5]. The anomalous shape of PC spectra above T_N can be associated with a large smearing of the density of states due to strong pair-breaking scattering which depresses the energy gap in the excitation spectrum [12]. Therefore, it is most likely that uncompensated spins of the spiral structure influence the superconductivity in a similar way as a high

concentration of magnetic impurities in conventional superconductors results in a gapless superconducting state [8,9].

From the reproducible PC spectra on various contacts, we were able to obtain a reliable determination of the temperature dependence of the superconducting order parameter $\Delta(T)$ in the Ho compound. The low temperature PC spectra can be described by the BTK theory for normal metal–superconductor point contacts [13]. The $dV/dI(V)$ curves have been fitted to the BTK formulas by varying the superconducting order parameter Δ and the dimensionless parameter Z for the barrier strength as well as the broadening parameter Γ [14]. The Γ parameter has been proposed by Dynes et al. [15] in order to include phenomenologically a broadening of the superconducting density of states in tunnel experiments. For a single crystal contact the results are presented in Fig. 1 (short-dashed lines) showing a good agreement with the experimental data at low bias voltages. The deviations at higher bias voltages (>4 mV) are explained by a (current induced) partial suppression of the superconductivity in the contact region. These structures are not reproducible between different contacts and do not contain any spectroscopic information.

The order parameter values fitted for a few typical contacts are plotted in Fig. 2 as a function of temperature. From a comparison with the theoretical BCS dependence $\Delta(T)$, a BCS transition temperature T_c^{BCS} at approximately 5.5–5.7 K is found below which a conventional superconducting state establishes. Using the order parameter values $\Delta(0) \simeq 0.8$–1.0 mV found for most contacts, one gets the characteristic ratio $2\Delta(0)/k_B T_c^{BCS} \simeq 3.2$–$4.2$ pointing to a moderate coupling strength for the largest ratios. Meanwhile, with a superconductivity onset temperature $T_c \simeq 8.5$ K, a ratio of about 2.4 is found which is anomalously small compared to the BCS value 3.5.

An indication for the temperature dependence of the order parameter in a wide temperature range can be obtained from the difference of the contact resistances in the normal and superconducting states ($R_n - R_s$) as shown in the insert to Fig. 2 for the contact presented in Fig. 1. According to the BTK theory, such a dependence is a qualitative measure for the temperature dependence of the order parameter provided that R_n is taken at zero bias and R_s at the gap

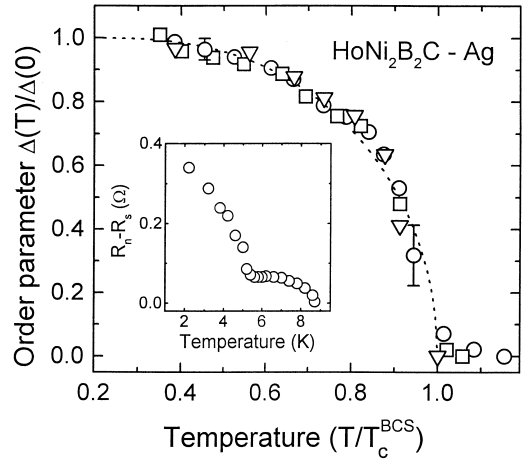

Fig. 2. Temperature dependences of the order parameter in normalized units for two polycrystal based contacts ($R(10\text{ mV}) \simeq 3.0\ \Omega$—squares, and $R(10\text{ mV}) \simeq 3.2\ \Omega$—circles), and a single crystal based contact ($R(10\text{ mV}) \approx 1.3\ \Omega$—triangles) with contact axis oriented along the *ab*-plane. Corresponding fitted values of the order parameters $\Delta(0)$ and the BCS transitions temperatures T_c^{BCS} are: 0.98 meV and 5.5 K (squares), 0.85 meV and 5.7 K (circles), 0.90 meV and 5.7 K (triangles). The BCS theoretical dependence is depicted by a dotted line. The insert shows the temperature dependence of a gap-related minimum, reproducing qualitatively the order parameter behavior over a wide temperature range for the contact presented in Fig. 1.

minimum position. The curve shown consists of two distinct branches merging together near T_N. An extrapolation of the low-temperature branch crosses the temperature axis in the vicinity of the apparent critical temperature $T_c^{BCS} \simeq 5.7$ K determined from the BCS fit for this contact. The temperature dependence of the pair density found via microwave experiments on $HoNi_2B_2C$ exhibits a narrow pronounced dip near T_N [16]. However, only a shallow minimum could be seen in our temperature dependence of the order parameter for single crystals around T_c^{BCS} (see the insert to Fig. 2). A reason for this dissimilarity is possibly associated with a smearing the superconducting density of states. Indeed, no evidence of such a minimum was found for polycrystalline samples where structural nonuniformity could increase this smearing.

The data presented prove the existence of two distinct types of superconductivity in $HoNi_2B_2C$ which manifest themselves in different temperature ranges [9]. Above T_c^{BCS}, the spectra give indications

for an anomalous gapless state, whereas a conventional BCS state develops only at lower temperatures. The full conversion of the anomalous spectra into BCS spectra at low temperatures proves that the magnetic phases of both the spiral structure and the AFM state develop in the same sample regions given by the contact size, unlikely the opposite assumption in Ref. [17].

4. Temperature dependence of the upper critical field

The field dependences of the zero-bias resistance $dV/dI(0,H)$ taken at various temperatures can be used to obtain the phase diagram $H_{c2}(T)$ [10]. Such a temperature set of $dV/dI(0,H)$ for a single-crystal based contact with the contact axis perpendicular to the *ab*-plane is given in Fig. 3, where the dashed and dotted lines reflect evidently the H_{c2} behavior in different temperature ranges. Similar curves could be also recorded for contacts with the contact axis directed along the *ab*-plane.

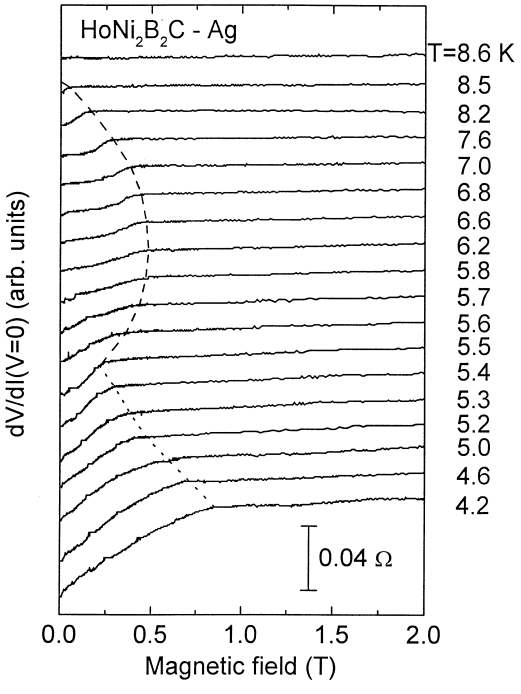

Fig. 3. Magnetic field dependences of the zero-bias resistance for the single crystal based $HoNi_2B_2C$–Ag contact ($R(1\ T) \simeq 1.1\ \Omega$) at different temperatures with the magnetic field and contact axis perpendicular to the *ab*-plane. The dashed and dotted lines follow the field position of the resistance saturation showing the reentrant behavior of H_{c2}. For clarity the curves are shifted vertically.

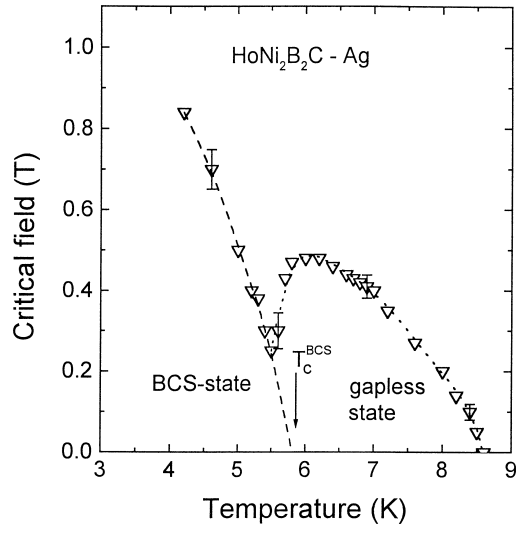

Fig. 4. The phase diagram $H_{c2}-T$ (open triangles) reconstructed from the data presented in Fig. 3. The low-temperature branch has been tentatively extrapolated to the critical temperature T_c^{BCS} of the BCS state. The dashed and dotted lines follow the data in the regions of the BCS and gapless states, respectively.

In Fig. 4, we have plotted the phase diagram $H_{c2}(T)$ reconstructed from the data presented in Fig. 3. The minimum seen in the diagram slightly above T_N is caused by a quasi-reentrance of the normal state, observed in transport and magnetization experiments [4–6]. The H_{c2} data at low temperatures have been tentatively extrapolated to the critical temperature $T_c^{BCS} = 5.8$ K as obtained from the temperature dependence of the $dV/dI(V)$ spectra for the given contact. The dashed and dotted curves indicate the possible existence of two branches in the $H_{c2}(T)$ diagram. We note that T_c^{BCS} is higher than the AFM transition temperature $T_N \sim 5.0$ K which shows that the BCS state, being associated with the AFM phase, originates already in the spiral spin state. This point implies that both structures develop in the same sample region probed by the point contact.

The minimum of $H_{c2}(T)$ in the vicinity of T_N was not always so pronounced as in Fig. 4. For the contacts based on polycrystal samples, the minimum

could be much smaller up to its full disappearance, resulting in plateau structure around T_N as reported in previous work [10]. From an analysis of PC data on the single crystal and polycrystalline samples a correlation was found between the strength of the reentrant structure in the $H_{c2}(T)$ dependence and the width of the tail in the $\Delta(T)$ curves near T_c^{BCS} (see Fig. 2). If the tail broadens significantly, the minimum in the $H_{c2}(T)$ curve becomes shallower and the plateau arises when the tail width reaches ~ 1 K. The reason is probably associated with some microvariations of the chemical composition over the sample volume, which leads to a broadening of the transition into the low temperature BCS state with possibly a smearing of the critical field dependence $H_{c2}(T)$ that obscures the quasi-reentrant behavior.

Estimating $H_{c2}(0)$ in the frame of the BCS theory from the slope dH_{c2}/dT near T_c, we get values in the range of 2–3 T. The main reason for the observed smaller critical fields at the lowest temperatures is evidently associated with a depairing effect of the antiferromagnetic phase. Magnetization and magnetoresistance measurements [5,6] gave H_{c2} values that are a few times smaller than the estimate from our point-contact data. To our knowledge, the largest critical field (of about 0.8 T at the lowest temperatures with an onset of superconductivity at 0.9 T) was observed by Krug et al. [18] in magnetoresitance data. The maximal value from our point-contact experiments at low temperatures (about 2 K) was near 1 T. The enhanced critical fields in the point-contact experiments can be related to surface effects (e.g., $H_{c3} = 1.69\ H_{c2}$) in a point-contact geometry. Besides, a point contact probes only a small sample region with possibly different superconducting properties compared to the average over a bulk sample.

5. Magnetic field dependence of the superconducting order parameter

On part of the point contacts investigated, we observed an unusually large increase of the gap voltage V_{min} at the minimum in the $dV/dI(V)$ spectra in modest magnetic fields (below $\sim 0.6\ H_{c2}$). Such a V_{min} shift could be seen for polycrystals as well as for single crystals with the magnetic field directed along *ab*-plane. The effect was repeatedly observed in more than ten contacts of different resistance with a well-defined Andreev-reflection current pointing to the genuine character of this phenomenon. Investigations on conventional BCS superconductors do not show such a shift of V_{min} (see, for instance, the magnetic-field dependent spectra of Nb and Sn in Ref. [19]). In some cases, the relative increase of V_{min} in a magnetic field for $HoNi_2B_2C$ occurred as large as 30%. No correlation of the V_{min} increase value with the PC resistance was found. A representative set of the $dV/dI(V)$ dependences is shown in Fig. 5 for different magnetic fields at 2.2 K, where the observed increase in the voltage position of the gap-structure related minima achieves namely 30% (insert of Fig. 5).

Due to the broadening of the spectra, the energy eV_{min} cannot be directly identified with the order parameter Δ. Moreover, the pair-breaking in a applied magnetic field will considerably enlarge the broadening. The dashed curves in Fig. 5 show the curves fitted by the BTK formulas taking account for an additional broadening by the introduction of a Γ parameter as discussed previously. In our phenomenological approach we include both the intrinsic broadening and magnetic-field induced broadening in the Γ parameter. The fitting procedure of the spectra cannot give unambiguous results by using three parameters (Δ, Γ, and Z), especially in the vicinity of H_{c2} where the broadening of the spectra is comparatively large. Therefore, the three parameters were determined from an analysis of the zero-field data. For the subsequent curves ($H < 0.8$ T), the Z parameter was kept constant.

The obtained relative enhancement of the order parameter in a magnetic field reached values up to $\sim 10\%$ as shown for a typical set of fitted Δ values in Fig. 6 together with two theoretical dependences. The dotted line presents a prediction of the Ginzburg–Landau phenomenological theory [20], strictly valid near T_c only. The second theoretical curve (solid line), valid in the whole temperature interval, is taken from the paper of Skalski et al. [12] assuming a linear magnetic-field dependence of the pair-breaking parameter $\alpha(H)$. It is very probable that the anomalous $\Delta(H)$ behavior in $HoNi_2B_2C$ is driven by the spin subsystem. In the following para-

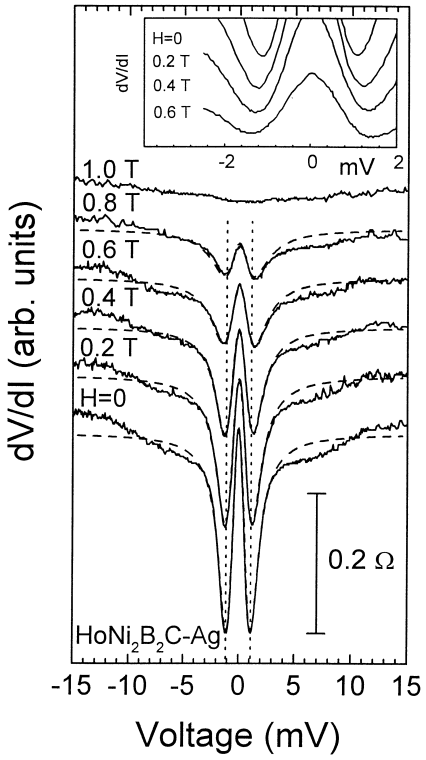

Fig. 5. The magnetic field effect on $dV/dI(V)$ curves (solid lines) of a single-crystal based $HoNi_2B_2C$–Ag contact ($R(10\ mV) \simeq 3.6\ \Omega$) with the magnetic field and contact axis oriented along the *ab*-plane, $T = 2.2$ K. The fields are indicated near each curve. BTK fits are displayed by dashed lines with scaling factors within 0.3–0.4 using the fitting parameters, from bottom to top: $\Delta = 1.04$, 1.09, 1.14, 1.12, and 0.74 meV; $\Gamma = 0.32$, 0.48, 0.54, 0.84, and 1.11 meV; $Z = 0.67$ for all the curves. The insert shows an enlarged view of the voltage position of the gap-related minima. For clarity the curves are shifted vertically.

graphs, we will consider possible reasons which could cause the order parameter enhancement in a magnetic field.

Fisher et al. [21] observed in the Ho-compound a large negative in-*ab*-plane longitudinal magnetoresistance in a wide temperature range above T_N, i.e., in the paramagnetic state. This phenomenon was explained by a decrease of the spin-disorder scattering due to the spin alignment in an applied magnetic field. Below T_N, a similar improved spin order could take place if some paramagnetism would occur in the low temperature range. Such a situation exists in the YNi_2B_2C system [22], where in spite of the nonmagnetic Y atoms evidence of paramagnetism is revealed over a wide temperature range.

Microwave experiments carried out on $HoNi_2B_2C$ have found an unknown source of magnetic pair-breaking below ~ 4 K [16]. This pair-breaking could be associated with the spiral spin structure of which, according to neutron-scattering data [3], residuals persist in the antiferromagnetic phase below T_N. The departure from a perfect AFM state can produce a net magnetic component on a scale comparable with ξ. Another possibility for uncompensated magnetic moments involves by rare-earth spins induced moments on the Ni sites, as it was found in the $ErNi_2B_2C$ compound [23]. An applied magnetic field suppresses the spin-disorder scattering from net magnetic moments as known from ferromagnets.

Thus, we assume that below T_N in $HoNi_2B_2C$, there is a significant pair-breaking effect due to deviations of the AFM structure from the perfect spin ordering or the appearance of other (fluctuating) magnetic contributions. In modest magnetic fields, the depairing effect of the magnetic moments can be reduced as a result of the improved spin alignment which compensates partially the direct depairing influence of the field. The interplay between these two opposite influences of the magnetic field defines the behavior of the superconducting order parameter in a magnetic field.

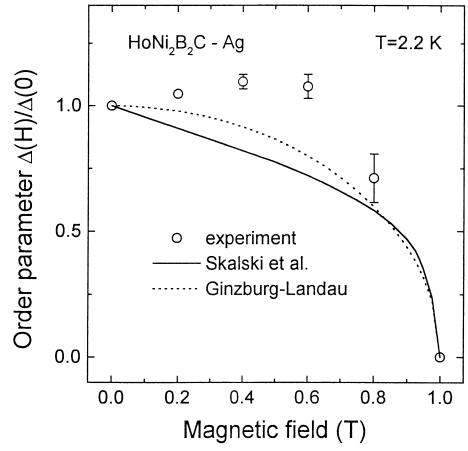

Fig. 6. A comparison of the magnetic field dependence of the order parameter $\Delta(H)$ (circles), determined from a BTK fit of the contact presented in Fig. 5, with two dependences following from pair-breaking theory.

6. Summary

From the point-contact studies on the magnetic superconductor $HoNi_2B_2C$ ($T_c \sim 8.5$ K) with an antiferromagnetic transition at $T_N \sim 5.0$ K, it has been found that a transition in the conventional BCS-like state takes place only at $T_c^{BCS} = 5.5–5.8$ K. Above T_c^{BCS}, the PC characteristics show evidence of gapless superconductivity. The gradual transformation of the two types of spectra near T_N suggests that both the incommensurate spiral magnetic structure and the antiferromagnetic state develop in the same probed contact area (dimension 10–100 nm) by varying the temperature.

The normal-state quasi-reentrance is seen as a pronounced dip in the $H_{c2}(T)$ dependence near T_N, but a few tenths of a degree below T_c^{BCS}. The BTK analysis of the spectra in a magnetic field yields an anomalous field-induced enhancement ($\sim 10\%$) of the superconducting order parameter. Probably, this effect is associated with an improved spin alignment in modest fields that reduce the pair-breaking scattering and increase the pair potential near the Ho sites.

Acknowledgements

We are grateful to Prof. I.K. Yanson for helpful discussions.

References

[1] R.J. Cava, H. Tagaki, H.W. Zandbergen, J.J. Krajewski, W.F. Peck Jr., T. Siegrist, B. Batlogg, R.B. van Dover, R.J. Felder, K. Mizuhashi, J.O. Lee, H. Eisaki, S. Uchida, Nature (London) 367 (1994) 252.
[2] A.I. Goldman, C. Stassis, P.C. Canfield, J. Zarestky, P. Dervenagas, B.K. Cho, D.C. Johnston, B. Sternlieb, Phys. Rev. B 50 (1994) 9668.
[3] T.E. Grigereit, J.W. Lynn, Q. Huang, A. Santoro, R.J. Cava, J.J. Krajewski, W.F. Peck Jr., Phys. Rev. Lett. 73 (1994) 2756.
[4] H. Eisaki, H. Tagaki, R.J. Cava, B. Batlogg, J.J. Krajewski, W.F. Peck Jr., K. Mizuhashi, J.O. Lee, S. Uchida, Phys. Rev. B 50 (1994) 647.
[5] P.C. Canfield, B.K. Cho, D.C. Johnston, D.K. Finnemore, M.F. Hundley, Physica C 230 (1994) 397.
[6] K.D.D. Rathnayaka, D.G. Naugle, B.K. Cho, P.C. Canfield, Phys. Rev. B 53 (1996) 5688.
[7] L.N. Bulaevskii, A.I. Buzdin, M.L. Kulic, S.V. Panjukov, Adv. Phys. 34 (1985) 175.
[8] A.A. Abrikosov, L.P. Gor'kov, Zh. Eksp. Teor. Fiz. 39 1960 1781 [Sovjet Phys.-JETP 12 (1961) 1243].
[9] L.F. Rybaltchenko, I.K. Yanson, A.G.M. Jansen, P. Mandal, P. Wyder, C.V. Tomy, D.McK. Paul, Europhys. Lett. 33 (1996) 483.
[10] L.F. Rybaltchenko, I.K. Yanson, A.G.M. Jansen, P. Mandal, P. Wyder, C.V. Tomy, D.McK. Paul, Physica B 218 (1996) 189.
[11] A.G.M. Jansen, A.P. van Gelder, P. Wyder, J. Phys. C 13 (1980) 6073.
[12] S. Skalski, O. Betbeder-Matibet, P.R. Weiss, Phys. Rev. 136 (1964) A1500.
[13] G.E. Blonder, M. Tinkham, T.M. Klapwijk, Phys. Rev. B 25 (1982) 4515.
[14] Y. de Wilde, T.M. Klapwijk, A.G.M. Jansen, J. Heil, P. Wyder, Physica B 218 (1996) 165.
[15] R.C. Dynes, V. Narayanamurti, J.P. Garno, Phys. Rev. Lett. 41 (1978) 1509.
[16] T. Jacobs, B.A. Willemsen, S. Sridhar, R. Nagarajan, L.C. Gupta, Z. Hossain, C. Mazumdar, P.C. Canfield, B.K. Cho, Phys. Rev. B 52 (1995) R7022.
[17] J.W. Lynn, Q. Huang, A. Santoro, R.J. Cava, J.J. Krajewski, W.F. Peck Jr., Phys. Rev. B 53 (1996) 802.
[18] K. Krug, M. Heinecke, K. Winzer, Physica C 267 (1996) 321.
[19] Yu.G. Naydiuk, R. Häussler, H.v. Löhneysen, Physica B 218 (1996) 122.
[20] V.L. Ginzburg, L.D. Landau, Zh. Eksp. Teor. Fiz. 20 (1950) 1064.
[21] I.R. Fisher, J.R. Cooper, P.C. Canfield, Phys. Rev. B 56 (1997) 10820.
[22] S.B. Roy, Z. Hossain, A.K. Pradhan, P. Chaddah, R. Nagarajan, L.C. Gupta, Physica C 256 (1996) 90.
[23] S.K. Sinha, J.W. Lynn, T.E. Grigereit, Z. Hossain, L.C. Gupta, R. Nagarajan, C. Godart, Phys. Rev. B 51 (1995) 681.